Neuropsychopharmacology (2014) 39, 866–874

www.neuropsychopharmacology.org

Imaging Nicotine- and Amphetamine-Induced Dopamine Release in Rhesus Monkeys with [^{11}C]PHNO *vs* [^{11}C]raclopride PET

Jean-Dominique Gallezot[1], Tracy Kloczynski[2], David Weinzimmer[1], David Labaree[1], Ming-Qiang Zheng[1], Keunpoong Lim[1], Eugenii A Rabiner[3], Khanum Ridler[3], Brian Pittman[2], Yiyun Huang[1], Richard E Carson[1,4], Evan D Morris[1,2,4] and Kelly P Cosgrove*[,1,2]

[1]Department of Diagnostic Radiology, Yale PET Center, Yale University School of Medicine, New Haven, CT, USA; [2]Department of Psychiatry, Yale University School of Medicine, New Haven, CT, USA; [3]GlaxoSmithKline, London, UK; [4]Department of Biomedical Engineering, Yale University School of Medicine, New Haven, CT, USA

The radiotracer [^{11}C]PHNO may have advantages over other dopamine (DA) D_2/D_3 receptor ligands because, as an agonist, it measures high-affinity, functionally active D_2/D_3 receptors, whereas the traditionally used radiotracer [^{11}C]raclopride measures both high- and low-affinity receptors. Our aim was to take advantage of the strength of [^{11}C]PHNO for measuring the small DA signal induced by nicotine, which has been difficult to measure in preclinical and clinical neuroimaging studies. Nicotine- and amphetamine-induced DA release in non-human primates was measured with [^{11}C]PHNO and [^{11}C]raclopride positron emission tomography (PET) imaging. Seven adult rhesus monkeys were imaged on a FOCUS 220 PET scanner after injection of a bolus of [^{11}C]PHNO or [^{11}C]raclopride in three conditions: baseline; preinjection of nicotine (0.1 mg/kg bolus + 0.08 mg/kg infusion over 30 min); preinjection of amphetamine (0.4 mg/kg, 5 min before radiotracer injection). DA release was measured as change in binding potential (BP_{ND}). Nicotine significantly decreased BP_{ND} in the caudate (7 ± 8%), the nucleus accumbens (10 ± 7%), and in the globus pallidus (13 ± 15%) measured with [^{11}C]PHNO, but did not significantly decrease BP_{ND} in the putamen or the substantia nigra or in any region when measured with [^{11}C]raclopride. Amphetamine significantly reduced BP_{ND} in all regions with both radiotracers. In the striatum, larger amphetamine-induced changes were detected with [^{11}C]PHNO compared with [^{11}C]raclopride (52–64% *vs* 33–35%, respectively). We confirmed that [^{11}C]PHNO is more sensitive than [^{11}C]raclopride to nicotine- and amphetamine-induced DA release. [^{11}C]PHNO PET may be more sensitive to measuring tobacco smoking-induced DA release in human tobacco smokers.

Neuropsychopharmacology (2014) **39,** 866–874; doi:10.1038/npp.2013.286; published online 13 November 2013

Keywords: nicotine; amphetamine; dopamine; non-human primate; PET; [^{11}C]PHNO

INTRODUCTION

Tobacco smoking continues to be a major health problem, with rates of smoking remaining steady at approximately 20% of the adult American population (CDC, 2010). Nicotine is the primary addictive chemical in tobacco smoke and exerts its initial reinforcing effects through the mesolimbic dopamine (DA) system(Di Chiara and Imperato, 1988). Specifically, nicotine releases DA by binding to $\alpha_4\beta_2$-nicotinic acetylcholine receptors located on the mesolimbic DA neurons in the ventral tegmental area, resulting in neuronal firing and DA release in the nucleus accumbens and dorsal caudate (Imperato *et al*, 1986). In preclinical microdialysis studies, acute doses of nicotine consistently increased DA by up to 200% from baseline (Brazell *et al*, 1990; Dewey *et al*, 1999; Di Chiara and Imperato, 1988; Gerasimov *et al*, 2000; Imperato *et al*, 1986).

Positron emission tomography (PET) imaging can also be used to examine drug-induced DA release. Drugs, such as amphetamine, increase synaptic DA, which competes with the radiotracer to bind at the DA receptor. An increase in DA results in a decrease in radiotracer binding compared with baseline. In this study, we measure this change in binding potential (BP_{ND}), which is an indirect measure of the change in synaptic DA. Amphetamine administration results in a reliable and robust increase in extracellular DA (~1000% increase from baseline in microdialysis studies) (Di Chiara and Imperato, 1988) and has been widely used in brain imaging studies to probe DA function (Laruelle, 2000; Slifstein *et al*, 2010). Attempts have also been made to measure nicotine- and tobacco smoking-induced DA release, but with inconsistent results.

*Correspondence: Dr KP Cosgrove, Department of Psychiatry, Yale University School of Medicine, 2 Church Street South, Suite 511, New Haven, CT 06519, USA, Tel: +1 203 737 6969, E-mail: kelly.cosgrove@yale.edu
Received 12 February 2013; revised 15 July 2013; accepted 16 July 2013; accepted article preview online 15 October 2013

In preclinical [^{11}C]raclopride studies nicotine challenges (ranging from 0.01 to 0.06 mg/kg, intravenously) resulted in 5–12% reductions in BP_{ND} in the caudate and putamen of monkeys (Dewey *et al*, 1999; Marenco *et al*, 2004). Similarly, a nicotine (0.05–0.5 mg/kg) challenge in pigs resulted in a 10% decrease in ventral striatal BP_{ND} (Cumming *et al*, 2003). Although an acute nicotine injection did not change [^{11}C]raclopride BP_{ND} in awake monkeys, BP_{ND} was reduced in anesthetized monkeys (Tsukada *et al*, 2002), suggesting that anesthetics routinely used in non-human primate imaging may confound data interpretation.

In humans, cigarette smoking consistently reduced [^{11}C]raclopride BP_{ND} by ~8% (Brody *et al*, 2006, 2009a, 2010) and up to 10% (Scott *et al*, 2007) in the ventral striatum in acutely abstinent tobacco smokers, but also see Barrett *et al* (2004). Note that nicotine alone may not be responsible for smoking-induced DA release. There are approximately 4000 chemicals in tobacco smoke, and one or more of these compounds may act alone or in concert with nicotine and the behavioral aspects of smoking to produce reinforcing and dopaminergic effects. For example, harman, an MAO inhibitor, may contribute to the reinforcing effects of cigarette smoking via a dopaminergic mechanism (Talhout *et al*, 2007; Villegier *et al*, 2007). Modest (~7%) reductions in [^{11}C]raclopride BP_{ND} were found using nicotine gum (Takahashi *et al*, 2007) but not nicotine nasal spray (Montgomery *et al*, 2007), indicating that nicotine administration may not produce DA release detectable with [^{11}C]raclopride PET.

The majority of PET studies examining DA release have used the radiotracer [^{11}C]raclopride, which is an antagonist, and binds to both high- and low-affinity D_2/D_3 receptors. However, the recently developed radiotracer [^{11}C]PHNO may have advantages over other D_2/D_3 receptor ligands because, as an agonist, it primarily measures the high-affinity, functionally active D_2/D_3 receptors that DA binds. Thus, it may be more sensitive to competition with endogenous DA (Narendran *et al*, 2006; Willeit *et al*, 2006, 2008). Improved sensitivity of [^{11}C]PHNO over [^{11}C]raclopride to amphetamine-induced changes in synaptic DA has been demonstrated (Ginovart *et al*, 2006; Shotbolt *et al*, 2012). Our objective was to take advantage of the sensitivity of [^{11}C]PHNO to measure the small DA signal induced by nicotine. In addition, [^{11}C]PHNO has a higher affinity for D3 *vs* D2 DA receptors, which allows for regional interpretation of D3 and D2 receptors (Girgis *et al*, 2011). Specifically, in human, binding in the dorsal striatum is primarily D2, binding in the substantia nigra is primarily D3, and binding in the globus pallidus is mixed with approximately 65% D3 *vs* D2 DA receptors (Tziortzi *et al*, 2011). This provides an additional advantage over [^{11}C]raclopride, which is constrained to the D2 DA receptor-rich areas in the striatum. In this study, we measured nicotine- and amphetamine-induced DA release in non-human primates with [^{11}C]PHNO *vs* [^{11}C]raclopride PET.

MATERIALS AND METHODS

Animals and Study Plan

Seven rhesus monkeys were included in the study (6 males, 1 female, body weight = 10.6 ± 3.3 kg, age = 6.7 ± 2.2 years). All experiments were conducted in accordance with the Yale University Institutional Animal Care and Use Committee guidelines. To avoid potential carryover effects of the radiotracer from one injection to the next, only one scan was performed per day and per animal. For the [^{11}C]PHNO study, all seven animals underwent one baseline scan; then, three animals underwent a retest scan, six animals underwent one postnicotine scan, and four animals underwent a postamphetamine scan. Five animals were included in the [^{11}C]raclopride study: all five animals underwent one baseline scan and one postnicotine scan, and four animals underwent one postamphetamine scan (Table 1).

Radiochemistry

[^{11}C]PHNO was prepared by *N*-acylation of the norpropyl precursor with [^{11}C]propionyl chloride followed by reduction of the resulting amide with lithium aluminum hydride and purification by reverse-phase HPLC, in a modified literature procedure similar to that used for the preparation of [^{11}C]NPA (Brown *et al*, 1997; Hwang *et al*, 2000; Wilson *et al*, 2005) as described previously (Gallezot *et al*, 2012). The purified [^{11}C]PHNO product was formulated in 1 ml of USP absolute ethanol and 10 ml of USP sterile saline. Filtration of the ethanolic saline solution through a 0.22 μm Millipore membrane filter produced a sterile apyrogenic

Table 1 Study Plan

	[^{11}C]PHNO				[^{11}C]Raclopride		
Animal	**Baseline**	**Retest**	**Nicotine challenge**	**Amphetamine challenge**	**Baseline**	**Nicotine challenge**	**Amphetamine challenge**
1	×	×	×				
2	×	×					
3	×		×	×	×	×	×
4	×		×	×	×	×	×
5	×	×	×	×	×	×	×
6	×		×	×	×	×	×
7	×		×		×	×	
n	7	3	6	4	5	5	4

[^{11}C]PHNO solution ready for intravenous administration. Radiochemical purity of the final product was >95%. The specific activity at end of synthesis was 77 ± 36 MBq/nmol ($n = 20$).

[^{11}C]Raclopride was prepared by C-11 methylation of the radiolabeling precursor desmethyl raclopride with [^{11}C]methyl triflate in the GE FxC-Pro automated synthesis module. The final product was formulated in 1 ml of USP absolute ethanol and 10 ml of USP sterile saline. Filtration of the ethanolic saline solution through a 0.22 μm Millipore membrane filter produced a sterile apyrogenic [^{11}C]raclopride solution ready for intravenous administration. Radiochemical purity of the final product was >95%. The specific activity at the end of synthesis was 264 ± 138 MBq/nmol ($n = 14$).

PET Imaging

Animals were initially anesthetized with ketamine hydrochloride (10 mg/kg, intramuscularly), transported to the PET facility, intubated, and maintained on oxygen and 1.5–4.0% isoflurane throughout the study. A 2-h interval was allowed between ketamine administration and injection of the radiotracer or drugs. Vital signs including respiration rate, blood pressure, heart rate, and temperature were monitored continuously and recorded every 15 min, and temperature was kept constant at 37 °C with heated water blankets. Arterial blood sampling was performed using a vascular access port, that is, a thin catheter leading from the femoral artery to a port implanted subcutaneously in the area of the hip, upper thigh, or dorsum, during a previous surgery. PET scans were performed on the Focus 220 PET scanner (Siemens/CTI, Knoxville, TN, USA), which has an intrinsic resolution of 1.4 mm at the center of the field of view. A transmission scan was acquired for image reconstruction.

Amphetamine and nicotine were obtained from Sigma Aldrich (St Louis, MO, USA). For amphetamine studies ($n = 8$), 0.4 mg/kg of amphetamine salt was administered as a 1-min bolus 5.0 ± 0.1 min before tracer injection. For nicotine studies ($n = 11$), 0.18 ± 0.01 mg/kg of nicotine was administered using a bolus-plus-infusion protocol started 21 ± 10 min before tracer injection. The bolus phase lasted 5 min (0.10 ± 0.01 mg/kg) and the infusion 32 ± 7 min (0.08 ± 0.01 mg/kg). Arterial blood samples were obtained for analysis of nicotine and cotinine or amphetamine at 2, 5, 15, 25 and 50 min after drug injection.

[^{11}C]PHNO (114 ± 45 MBq) or [^{11}C]raclopride (174 ± 21 MBq) was injected in a 3-min bolus using a syringe pump (Harvard PHD 22/2000; Harvard Apparatus, Holliston, MA), and list-mode data were acquired for 120 min. The injected mass was 0.08 ± 0.02 μg/kg (max 0.1 μg/kg) for [^{11}C]PHNO and 0.08 ± 0.02 μg/kg (max 0.2 μg/kg) for [^{11}C]raclopride.

Dynamic scan data were binned into a sequence of 33 frames (6 × 30 s; 3 × 1 min; 2 × 2 min; 22 × 5 min), and each frame was reconstructed with the appropriate corrections (attenuation, normalization, scatter, randoms, and dead-time), using a FORE/FBP algorithm and a Shepp filter with a cutoff frequency of 0.15 times the sampling frequency (reconstructed image resolution approximately 3.2 mm).

Arterial Input Function Measurement for [^{11}C]PHNO

The arterial input function was measured for 16 out of 20 PET studies performed with [^{11}C]PHNO, and was used to validate the selection of kinetic model to quantify [^{11}C]PHNO BP_{ND} (see Supplementary Information for details).

MR Imaging

MR images were acquired for each rhesus monkey on a Siemens 3.0 T Trio scanner, using an extremity coil. T1-weighted images were acquired in the coronal plane with a spin echo sequence (TE = 3.34, TR = 2530, flip angle = 7°, section thickness = 0.50 mm, field of view = 140 mm, image matrix = 256 × 256 × 176 pixels, matrix size = 0.547 × 0.547 × 0.500 mm^3). Non-brain tissue was removed and the image cropped to 176 × 176 × 176 pixels using MEDx software (Medical Numerics, Germantown, MD) before coregistration with PET images.

Region of Interest Delineation

An existing region of interest (ROI) map defined on a template brain (a representative MR image of a brain, from an animal not included in the study) was utilized. The following, *a priori* defined, ROIs were examined: cerebellum (5.9 cm^3), caudate (0.43 cm^3), putamen (0.38 cm^3), globus pallidus (0.13 cm^3), nucleus accumbens (0.09 cm3), and substantia nigra (0.10 cm^3). Both [^{11}C]PHNO and [^{11}C]raclopride were used to measure BP_{ND} in the caudate, putamen, and nucleus accumbens. Owing to low raclopride signal, only [^{11}C]PHNO has measurable BP_{ND} in the globus pallidus and substantia nigra. Similarly, although [^{11}C]PHNO has moderate binding in the thalamus ($BP_{ND} \sim 0.3$), this region was not part of our primary hypothesis and was excluded *a priori* to avoid reducing statistical power (due to multiple comparisons) in higher binding regions. The regions were drawn on coronal slices on the template MR image. In particular, the substantia nigra was drawn on seven consecutive slices in the midbrain with location and shape of the ROI based on a histological atlas (Paxinos *et al*, 2000). The cerebellum ROI includes both gray and white matter tissues. A nonlinear transformation was used (bioimagesuite program; version 2.5; http://www.bioimagesuite.org/) to transfer the ROI template to the MR image of each subject. Then, the MR and PET images of each monkey were coregistered using a rigid body registration using an automatically selected PET sum image (Sandiego *et al*, 2013).

Kinetic Modeling

[^{11}C]raclopride BP_{ND} were quantified using the simplified reference tissue model (SRTM) (Lammertsma and Hume, 1996) using the cerebellum time–activity curve (TAC) as input data. The SRTM operational equation is:

$$C_T(t) = R_1 C_{Ref}(t) + R_1\left(k_2' - k_2\right) C_{Ref}(t) \otimes e^{-k_2 t}$$

where R_1 is the relative influx rate in the target region, k_2 and k_2' are the efflux rates from the target and reference regions, respectively, and BP_{ND} is equal to $R_1 k_2'/k_2 - 1$.

[^{11}C]PHNO BP_{ND} (Innis *et al*, 2007) were quantified using the multilinear analysis MA1 (Ichise *et al*, 2002) using the arterial input function, and the cerebellum as reference region to estimate the non-displaceable volume of distribution (V_{ND}). MA1 is based on the graphical analysis (Logan *et al*, 1990). As arterial input functions were not available for all [^{11}C]PHNO studies, binding potentials BP_{ND} were also estimated using two reference region methods: SRTM and MRTMS, both using the cerebellum TAC as input data. This second reference method is a simplification of the multilinear methods MRTM and MRTM2 (Ichise *et al*, 2008; Ichise *et al*, 2002). MRTMS differs from MRTM and MRTM2 in that it drops a term on the right-hand side of the equation directly proportional to the reference tissue concentration. This approach is based on the same hypotheses as the simple form of reference region graphical analysis (Gunn *et al*, 2002; Logan *et al*, 1996; see equation 7). The MRTMS, operational equation is:

$$C_T(t) = -\frac{1+BP_{ND}}{b}\int_0^t C_{Ref}(u)du + \frac{1}{b}\int_0^t C_T(u)\,du,\ tt^*$$

where C_T and C_{Ref} represent the target ROI and the cerebellum TACs, respectively. The time t^* after which the underlying graphical analysis plot is considered linear was set to 20 min for MA1 and 40 min for MRTMS.

Statistical Analysis

Test–retest variability (TRV) of [^{11}C]PHNO BP_{ND} was assessed by computing the mean and standard deviation of

$$2\times\left(BP_{ND}^{Scan2}-BP_{ND}^{Scan1}\right)/\left(BP_{ND}^{Scan2}+BP_{ND}^{Scan1}\right).$$

Linear mixed models were used to examine changes in BP_{ND} levels across drug and region. Separate models were developed for each radiotracer with three regions (caudate, putamen, nucleus accumbens) and five regions (caudate, putamen, nucleus accumbens, globas pallidus, substantia nigra) included in the [^{11}C]raclopride and [^{11}C]PHNO models, respectively. In these models, both drug (baseline, nicotine, amphetamine) and region were modeled as within-subjects factors. Within-subject correlations were accounted for with random subject effects and by fitting the best variance–covariance structure to the data according to the Bayesian Information Criterion. For the [^{11}C]PHNO model, separate variance and covariance parameters were estimated within each region, based on regional heterogeneity. Owing to the limited size of the current sample, we report unadjusted p-values ($p<0.05$). Spearman's correlations were used to examine relationships between changes in BP_{ND} and plasma levels of nicotine and amphetamine. Statistical calculations were performed using SAS, version 9.3 (SAS, Cary, NC).

Effect size was computed as the absolute value of the mean difference of the BP_{ND}, before and after drug (either nicotine or amphetamine), divided by the standard deviation of the differences. Statistical power computations were performed using G*Power 3 (version 3.1.6), using a power (β) of 0.8 and an error probability (α) of 0.05, and a one-tailed hypothesis, as in a previous study with nicotine and [^{11}C]raclopride (Marenco *et al*, 2004).

RESULTS

Quantification of [^{11}C]PHNO BP_{ND}

[^{11}C]PHNO binding potentials BP_{ND} estimated with MA1 and arterial input function and MRTMS with the cerebellum as input were highly correlated ($y=0.893x+0.244$, $r^2=0.962$, 16 scans and 5 regions of interest). SRTM BP_{ND} showed a lower slope in its regression relationship with MA1 BP_{ND} ($y=0.786x+0.549$, $r^2=0.961$). Therefore, MRTMS BP_{ND} estimates were selected to evaluate the TRV of [^{11}C]PHNO binding, and the effects of nicotine and amphetamine on [^{11}C]PHNO binding, including all studies (with and without arterial blood sampling) (see Supplementary Information for details).

TRV of [^{11}C]PHNO BP_{ND}

The average [^{11}C]PHNO BP_{ND} obtained during the three test scans of the test–retest study, and the relative changes in BP_{ND} between the test and retest scans are shown in Table 2. The test and retest BP_{ND} estimates were not significantly different in any region (paired Student's t-test, the smallest p-value was 0.12, in the substantia nigra). The TRV of BP_{ND}, estimated as the standard deviation of the difference in BP_{ND}, ranged from 6% in the nucleus accumbens to 17% in the caudate and substantia nigra.

Plasma Levels of Nicotine and Amphetamine

Amphetamine levels (ng/ml) in the blood peaked rapidly at 391 ± 26 (2 min), and then progressively declined as follows: 192 ± 28 (5 min), 133 ± 23 (15 min), 112 ± 19 (25 min), and 94 ± 19 (50 min). Areas under the curve (until 50 min) for all amphetamine studies were $6305+834$ ng/ml · min. Nicotine levels (ng/ml) in the blood were as follows: 127 ± 47 (2 min), 176 ± 48 (5 min), 64 ± 15 (15 min), 65 ± 10 (25 min), and 31 ± 6 (50 min) consistent with a bolus plus constant infusion administration. Areas under the curve (until 50 min) for all nicotine studies were $4044+737$ ng/ml · min. Levels of cotinine (ng/ml), the major metabolite of nicotine, in the blood were as follows: 0.7 ± 1.2 (2 min), 21 ± 19 (5 min), 57 ± 24 (15 min), 77 ± 23 (25 min), and 104 ± 25 (50 min).

Nicotine- and Amphetamine-Induced BP_{ND} Changes with [^{11}C]PHNO

The effects of the nicotine and amphetamine on [^{11}C]PHNO BP_{ND} are presented in Table 3 and Figure 1. There was a

Table 2 [^{11}C]PHNO Binding Potentials and Test–Retest Variability ($n=3$)

	BP_{ND}	ΔBP_{ND} (%)
Caudate	3.8 ± 0.6	7 ± 17
Putamen	4.5 ± 0.1	−2 ± 10
N. acc	5.0 ± 0.8	−3 ± 6
GP	6.5 ± 0.9	6 ± 14
S. nigra	4.3 ± 1.6	2 ± 17

Abbreviations: GP, globus pallidus; N. acc, nucleus accumbens; S. nigra, substantia nigra.

Table 3 Effect of Nicotine and Amphetamine on [^{11}C]PHNO BP_{ND}

	Nicotine ($n=6$)			Amphetamine ($n=4$)			*Post hoc* test (*$p<0.05$)		Effect size	
	Baseline	Nicotine	ΔBP_{ND} (%)	Baseline	Amphetamine	ΔBP_{ND} (%)	Baseline *vs* nicotine	Baseline *vs* amphetamine	Baseline *vs* nicotine	Baseline *vs* amphetamine
Caudate	4.0 ± 0.5	3.7 ± 0.6	− 7 ± 8	3.8 ± 0.5	1.8 ± 0.3	− 52 ± 2	*	*	0.96	11.
Putamen	4.5 ± 0.6	4.2 ± 0.8	− 6 ± 10	4.5 ± 0.7	2.1 ± 0.6	− 53 ± 10	NS	*	0.61	4.7
N. acc.	5.2 ± 0.9	4.6 ± 0.5	− 10 ± 7	4.8 ± 0.7	1.7 ± 0.3	− 64 ± 6	*	*	1.20	4.2
GP	7.0 ± 0.6	6.1 ± 1.0	− 13 ± 15	7.2 ± 0.3	5.1 ± 0.3	− 29 ± 6	*	*	0.87	4.0
S. nigra	4.3 ± 0.9	4.1 ± 0.7	− 2 ± 24	4.4 ± 1.1	2.1 ± 0.3	− 50 ± 14	NS	*	0.17	1.9

Abbreviations: GP, globus pallidus; N. acc, nucleus accumbens; NS, not significant; S. nigra, substantia nigra.
*Denotes significant $p<0.05$.

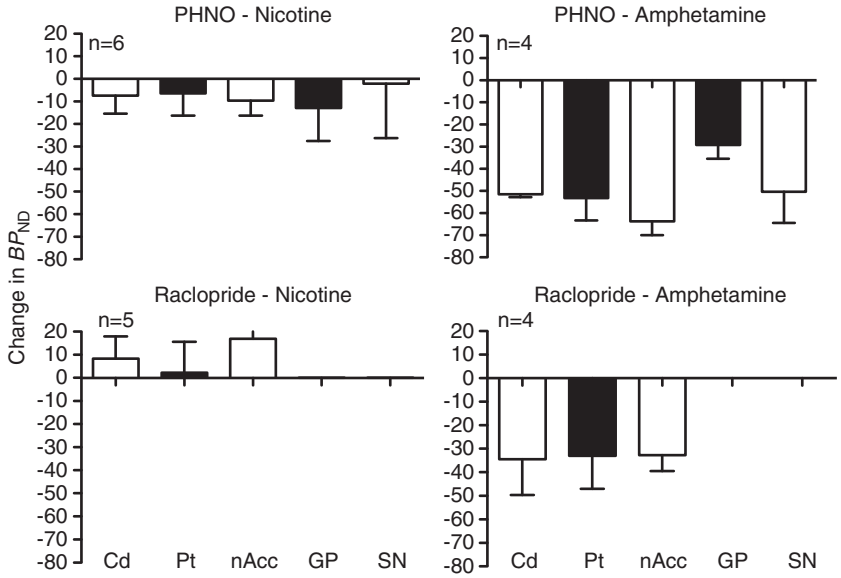

Figure 1 Change in BP_{ND} is pictured for nicotine- (left panels) and amphetamine- (right panels) induced DA release using [^{11}C]PHNO (upper panels) and for [^{11}C]raclopride (lower panels) in the caudate (Cd), putamen (Pt), nucleus accumbens (nAcc) for both tracers and for globus pallidus (GP) and substantia nigra (SN) for [^{11}C]PHNO.

significant main effect of drug ($F(2,8)\geqslant 89$, $p<0.0001$). *Post hoc* tests indicate that amphetamine significantly reduced BP_{ND} ($p<0.0001$) in all regions (-29 ± 6 to $-64\pm6\%$), and nicotine significantly reduced BP_{ND} in the caudate ($-7\pm8\%$, $p=0.02$), the nucleus accumbens ($-10\pm7\%$, $p=0.006$), and the globus pallidus ($-13\pm15\%$, $p=0.04$) but not in the putamen ($p=0.14$) or the substantia nigra ($p=0.68$). The effect size was lowest in the substantia nigra (0.17 for nicotine and 1.9 for amphetamine), and highest in the caudate for amphetamine (11.0) and in the nucleus accumbens for nicotine (1.20).

Nicotine- and Amphetamine-Induced BP_{ND} Changes with [^{11}C]raclopride

The effects of nicotine and amphetamine on [^{11}C]raclopride BP_{ND} are presented in Table 4 and Figure 1. In the caudate, putamen, and nucleus accumbens, where there is measurable [^{11}C]raclopride BP_{ND}, the main effect of drug was significant ($F(2,29)\geqslant 14.6$, $p<0.0001$). *Post hoc* tests indicate that amphetamine significantly reduced BP_{ND} ($p<0.01$) in all three regions (-33 ± 7 to $-35\pm15\%$), whereas nicotine did not significantly reduce BP_{ND} in any region (2 ± 13 to$17\pm16\%$). There was a significant increase in BP_{ND} in the nucleus accumbens ($p<0.01$). This is partially because, in one monkey, nicotine resulted in increased BP_{ND} in all regions (25% in the putamen to 38% in the nucleus accumbens) and this was not consistent with the other four animals across regions ($-2\pm9\%$ in the putamen to $12\pm13\%$ in the nucleus accumbens). Owing to the variable and unexpected direction of the change of BP_{ND} with nicotine, the effect size was only computed for amphetamine studies. The effect size was 2.0 in the caudate and putamen and 4.5 in the nucleus accumbens.

Comparison of [^{11}C]PHNO and [^{11}C]raclopride sensitivity to the Amphetamine Challenge

ΔBP_{ND} estimates induced by amphetamine tended to be larger for [^{11}C]PHNO than for [^{11}C]raclopride in all regions, and this difference was significant in the nucleus accumbens

Table 4 Effect of Nicotine and Amphetamine on [^{11}C]Raclopride BP_{ND}

	Nicotine ($n=5$)			Amphetamine ($n=4$)			*Post hoc* test (*$p<0.05$)		Effect size	
	Baseline	Nicotine	ΔBP_{ND} (%)	Baseline	Amphetamine	ΔBP_{ND} (%)	Baseline *vs* nicotine	Baseline *vs* amphetamine	Baseline *vs* nicotine	Baseline *vs* *amph*etamine
Caudate	3.8 ± 0.4	4.1 ± 0.7	8 ± 10	3.7 ± 0.3	2.4 ± 0.5	− 35 ± 15	NS	*	NC	2.0
Putamen	5.3 ± 0.6	5.4 ± 1.1	2 ± 13	5.2 ± 0.7	3.5 ± 0.9	− 33 ± 14	NS	*	NC	2.0
N. acc.	2.2 ± 0.2	2.6 ± 0.2	17 ± 16	2.2 ± 0.1	1.5 ± 0.1	− 33 ± 7	*	*	NC	4.5

Abbreviations: N. acc., nucleus accumbens; NC, not computed; NS, not significant.

(paired Student's *t*-test, $p<0.001$) but not in the caudate ($p=0.09$) or putamen ($p=0.25$).

Relationships Between ΔBP_{ND} and Plasma Variables

For correlation analyses, results from [^{11}C]PHNO and [^{11}C]raclopride were grouped. There were no significant correlations between peak nicotine or amphetamine concentration, nicotine or amphetamine AUC and ΔBP_{ND}. There was a trend toward a negative relationship between ΔBP_{ND} in the putamen with nicotine AUC ($p=0.08$, $r=-0.49$) and peak nicotine concentration ($p=0.07$, $r=-0.53$) suggesting a larger percent change in BP_{ND} with increasing nicotine plasma concentrations.

DISCUSSION

In the current study, we found statistically significant nicotine-induced DA release in the striatum with [^{11}C]PHNO but not [^{11}C]raclopride PET. As expected, amphetamine-induced striatal DA release was robust and reliably and significantly measured with both [^{11}C]raclopride (33–35%) and [^{11}C]PHNO (52–64%). Nicotine caused a detectable amount of DA release in the caudate (7%), nucleus accumbens (10%), and an extrastriatal region, the globus pallidus (13%), as measured with [^{11}C]PHNO. We did not find significant relationships between plasma amphetamine or nicotine concentrations and ΔBP_{ND} with either radiotracer.

Nicotine produced small (6–10%) but significant reductions in striatal BP_{ND} with [^{11}C]PHNO and variable increases (2–17%) in striatal BP_{ND} with [^{11}C]raclopride. Our findings with [^{11}C]PHNO are in line with the human literature suggesting that tobacco smoking results in ~8% reduction in BP with [^{11}C]raclopride (Brody *et al*, 2010, 2009a, b; Scott *et al*, 2007) and are also consistent with the preclinical literature reporting small but significant (5–10%) reductions in [^{11}C]raclopride BP_{ND} by intravenous nicotine (0.06–0.5 mg/kg, intravenously) (Cumming *et al*, 2003; Marenco *et al*, 2004). In our hands, [^{11}C]PHNO TRV was higher at 7 + 17% in the caudate and 2 + 10% in the putamen based on data from three monkeys. This suggests that a 6–10% reduction in [^{11}C]PHNO BP_{ND} by nicotine is not greater than the variability we find in the current study within baseline [^{11}C]PHNO scans. A limitation is that the current study may have been underpowered to detect a larger effect in the striatum and studies involving human subjects will have larger sample sizes. In fact, the effect sizes in the nicotine experiments with [^{11}C]PHNO in the current study were similar (putamen) or higher (other basal ganglia ROIs) than the effect size reported previously (Marenco *et al*, 2004) using [^{11}C]raclopride (0.62).

[^{11}C]PHNO BP_{ND} values were quantified using MRTMS. In humans, SRTM (Lammertsma and Hume, 1996) and the simple form of the noninvasive graphical analysis (Gunn *et al*, 2002; Logan *et al*, 1996; equation 7) can be used to quantify [^{11}C]PHNO BP_{ND} without arterial blood sampling (Ginovart *et al*, 2007b). However, in the current study, in rhesus monkeys SRTM tended to underestimate [^{11}C]PHNO BP_{ND}, especially in regions with high BP_{ND} values (eg, in the pallidum SRTM BP_{ND} values were 15 ± 4% lower than with MA1). SRTM has not previously been extensively compared with methods using arterial blood sampling in rhesus monkeys. This underestimation may be due the higher BP_{ND} values observed in rhesus monkeys (7.0 ± 0.6 in the pallidum) than in humans (mean pallidum BP_{ND} values were within the 3–4 range depending on the method (Ginovart *et al*, 2007a). MRTMS, which is based on the same hypotheses as the simple form of the noninvasive graphical analysis, but reduces the noise-induced bias seen in the graphical analyses like the MRTM and MRTM2 methods, provided [^{11}C]PHNO BP_{ND} estimates that were better correlated with BP_{ND} values obtained using arterial blood sampling. MRTMS is similar to MRTM, but one less parameter needs to be estimated in MRTMS, which can help reduce the variability of BP_{ND} estimates. Conversely, MRTMS is applicable to fewer tracers than MRTM or MRTM2, in the same manner that the simpler form of the noninvasive graphical analysis (Gunn *et al*, 2002; Logan *et al*, 1996; equation 7) is applicable in fewer cases than the three-parameter form (Ichise *et al*, 1996; Logan *et al*, 1996; equation 6).

The injected mass of [^{11}C]PHNO used in this study (0.08 μg/kg) is below the tracer dose limit for D_2 receptors but not for D_3 receptors. In humans, the recommended dose of [^{11}C]PHNO is 0.029 μg/kg or lower, to reduce the frequency of side effects (Mizrahi *et al*, 2010). The true tracer dose of [^{11}C]PHNO at D_3 receptors may be lower still. In anesthetized rhesus monkeys, the tracer dose limit may be higher than in humans as the uptake of [^{11}C]PHNO is lower in the cerebellum of anesthetized rhesus monkeys than in humans. The average SUV at 60–120 min after injection in the cerebellum measured in our laboratory was 0.36 ± 0.06 ($n=34$ baseline scans) and 0.63 ± 0.10 ($n=48$ baseline scans) in rhesus monkeys and humans, respectively. We estimated that the tracer dose in rhesus monkeys is 0.01–0.02 μg/kg (for 5% occupancy) in a previous study

(Gallezot *et al*, 2012). Based on that study, the self-occupancy of [^{11}C]PHNO at D_3 receptors would be 25% in this study. This would reduce the effect of nicotine. For example, if the true occupancy of nicotine were 10% for D_3 receptors, the D3-related observed effect would be only 7.6%. However, specific activities achievable for [^{11}C]PHNO are lower than that of [^{11}C]raclopride owing to the more complicated synthesis. We decided to use a higher than tracer dose as a trade-off to reduce the noise in PET images.

The dose of nicotine (0.18 mg/kg over 30 min) used in this study was based on earlier work by Domino and Tsukada (2009) that reported a 300% increase in striatal DA above baseline measured with microdialysis in awake monkeys. The increase was sustained for over 2 h, suggesting that we did not miss a transient change in DA. It is possible that increases in extrasynaptic DA measured by microdialysis do not directly reflect changes in synaptic DA levels and the paradigm chosen may not have been optimal to measure changes in synaptic levels of DA. The aim of the study was to elicit maximal DA release to determine if it could be reliably measured with [^{11}C]raclopride or [^{11}C]PHNO. Earlier preclinical studies using bolus nicotine administration (Cumming *et al*, 2003; Dewey *et al*, 1999; Marenco *et al*, 2004), which more closely resemble human smoking, did not find larger changes in BP_{ND} than ours. Those papers reported changes on the order of 5–10%, similar to our findings.

Even though an initial human smoking study reported relatively large changes in BP_{ND} (Brody *et al*, 2004), follow-up studies by the same group concluded that smoking a cigarette causes an approximate 8% reduction in BP_{ND}. These findings are generally consistent with the preclinical studies reviewed above. We note one important difference between the human and animal studies is that the humans are nicotine-dependent. Interestingly, microdialysis studies suggest slightly greater nicotine-induced DA release in nicotine pre-treated *vs* saline-treated animals (Marshall *et al*, 1997; Shim *et al*, 2001). Thus, it is possible that smoking-induced DA release is somewhat greater in nicotine-dependent subjects compared with the preclinical studies. We are currently developing and evaluating alternative methods for measuring smoking-induced DA release in chronic human tobacco smokers (Morris *et al*, 2013; Sullivan *et al*, 2013). These methods are designed to detect brief DA changes that may be localized to subregions of the striatum.

In addition to finding significant reductions in striatal BP_{ND} with nicotine and [^{11}C]PHNO, there was a significant reduction in [^{11}C]PHNO BP_{ND} in the globus pallidus, which has not been reported previously. The majority of studies investigating DA release use the radiotracer [^{11}C]raclopride, which measures D_2/D_3 receptors, in the caudate and putamen, but [^{11}C]PHNO allows for additional measurement of D_2/D_3 receptors in the globus pallidus and substantia nigra, which contain predominantly D_3 receptors. The DA neurons in the globus pallidus are primarily involved in voluntary motor function. However, DA release in the globus pallidus in response to food presentation and consumption has been measured with microdialysis in rodents(Fuchs *et al*, 2005; Hauber and Fuchs, 2000). This suggests a role for the globus pallidus in appetitive behavior, which may include drug abuse. Although amphetamine administration (0.42 mg/kg, *per os*) to humans did not significantly reduce [^{11}C]PHNO BP_{ND} in the globus pallidus (6.5%), we found a significant reduction (29%) with amphetamine (0.4 mg/kg, intravenously) in anesthetized non-human primates. The difference in results may be due to the differences in the route of administration or to anesthesia.

[^{11}C]PHNO has been shown to have greater sensitivity over [^{11}C]raclopride to amphetamine-induced striatal DA release in healthy human (Shotbolt *et al*, 2012) and in cat brain(Ginovart *et al*, 2006). Our findings support increased sensitivity of [^{11}C]PHNO over [^{11}C]raclopride, for amphetamine (52–64% *vs* 25–33%, respectively). In addition, we obtained a more reliable and significant signal with [^{11}C]PHNO when measuring small changes in DA induced by nicotine. Unlike [^{11}C]raclopride, [^{11}C]PHNO can be used to measure binding in D_3-rich regions, such as the globus pallidus and substantia nigra. As DA has higher affinity for D_3 receptors, a given amount of released DA would produce a larger change in the globus pallidus than in the caudate or putamen. This may be a contributing factor to our ability to detect a significant nicotine-induced change in the pallidum. As for PHNO in the substantia nigra, which is effectively all D_3, this region's small size in combination with a relatively less robust effect of nicotine *vs* amphetamine on DA release, makes reliable detection of changes more difficult. The two other regions with the highest ratio of D_3 to D_2 receptors (pallidum, nucleus accumbens) are also intrinsically small and suffer from partial volume effects, with both spill-out of the signal outside of the region and spill in for neighboring D2-rich regions. This would reduce the benefits of being able to observe both D_2 and D_3 receptors with [^{11}C]PHNO. In future studies, improvement in specific activities or improvement in reconstruction algorithms and noise reduction techniques may help to obtain higher resolution images. In human studies, the relative size of brain ROIs compared with the scanner resolution may be more favorable, especially since with the filtering included in the FBP algorithm in the current study, the resolution of the images (about 3.2 mm) is not much higher than that of the best dedicated brain scanners for human studies.

In the current study, we detected significant striatal (caudate and nucleus accumbens) DA release induced by nicotine with [^{11}C]PHNO but not [11C]raclopride PET. BP_{ND} in the globus pallidus, an extra-striatal region, as measured with [^{11}C]PHNO was also significantly reduced. In addition, we replicated the recent finding that [^{11}C]PHNO is more sensitive than [^{11}C]raclopride for measuring amphetamine-induced DA release. Thus, [^{11}C]PHNO PET may be more sensitive than [^{11}C]raclopride for measuring tobacco smoking-induced DA release in human tobacco smokers.

FUNDING AND DISCLOSURE

This publication was made possible by NIH Grants R03DA025820, K01DA20651, and K02DA031750 (KPC). This publication was also made possible by CTSA Grant Number UL1 RR024139 from the National Center for Research Resources (NCRR) and the National Center for Advancing Translational Science (NCATS), components of

the National Institutes of Health (NIH), and NIH roadmap for Medical Research. Its contents are solely the responsibility of the authors and do not necessarily represent the official view of NIH.

ACKNOWLEDGEMENTS

The authors acknowledge the expertise of the staff of the Yale PET Center.

REFERENCES

Barrett SP, Boileau I, Okker J, Pihl RO, Dagher A (2004). The hedonic response to cigarette smoking is proportional to dopamine release in the human striatum as measured by positron emission tomography and [^{11}C]raclopride. *Synapse* **54**: 65–71.

Brazell MP, Mitchell SN, Joseph MH, Gray JA (1990). Acute administration of nicotine increases the *in vivo* extracellular levels of dopamine, 3,4-dihydroxyphenylacetic acid and ascorbic acid preferentially in the nucleus accumbens of the rat: comparison with caudate–putamen. *Neuropharmacology* **29**: 1177–1185.

Brody AL, London ED, Olmstead RE, Allen-Martinez Z, Shulenberger S, Costello MR *et al* (2010). Smoking-induced change in intrasynaptic dopamine concentration: effect of treatment for tobacco dependence. *Psychiatry Res* **183**: 218–224.

Brody AL, Mandelkern MA, Olmstead RE, Allen-Martinez Z, Scheibal D, Abrams AL *et al* (2009a). Ventral striatal dopamine release in response to smoking a regular *vs* a denicotinized cigarette. *Neuropsychopharmacology* **34**: 282–289.

Brody AL, Mandelkern MA, Olmstead RE, Scheibal D, Hahn E, Shiraga S *et al* (2006). Gene variants of brain dopamine pathways and smoking-induced dopamine release in the ventral caudate/nucleus accumbens. *Arch Gen Psychiatry* **63**: 808–816.

Brody AL, Olmstead RE, Abrams AL, Costello MR, Khan A, Kozman D *et al* (2009b). Effect of a history of major depressive disorder on smoking-induced dopamine release. *Biol Psychiatry* **66**: 898–901.

Brody AL, Olmstead RE, London ED, Farahi J, Meyer JH, Grossman P *et al* (2004). Smoking-induced ventral striatum dopamine release. *Am J Psychiatry* **161**: 1211–1218.

Brown DJLuthra SKBrady FPrenant CDijkstra DWikstrom H (eds) (1997). Labelling of the D2-agonist-(+)-PHNO using [^{11}C]-propionyl chloride. *Proceedings of the XIIth International Symposium on Radiopharmaceutical Chemistry*. John Wiley and Sons: Uppsala, Sweden.

CDC (2010). Vital signs: current cigarette smoking among adults aged >/=18 years—United States, 2005–2010. *Morb Mortal Wkly Rep* **60**: 1207–1212.

Cumming P, Rosa-Neto P, Watanabe H, Smith D, Bender D, Clarke PB *et al* (2003). Effects of acute nicotine on hemodynamics and binding of [^{11}C]raclopride to dopamine D2,3 receptors in pig brain. *Neuroimage* **19**: 1127–1136.

Dewey SL, Brodie JD, Gerasimov M, Horan B, Gardner EL, Ashby CR Jr (1999). A pharmacologic strategy for the treatment of nicotine addiction. *Synapse* **31**: 76–86.

Di Chiara G, Imperato A (1988). Drugs abused by humans preferentially increase synaptic dopamine concentrations in the mesolimbic system of freely moving rats. *Proc Natl Acad Sci USA* **85**: 5274–5278.

Domino EF, Tsukada H (2009). Nicotine sensitization of monkey striatal dopamine release. *Eur J Pharmacol* **607**: 91–95.

Fuchs H, Nagel J, Hauber W (2005). Effects of physiological and pharmacological stimuli on dopamine release in the rat globus pallidus. *Neurochem Int* **47**: 474–481.

Gallezot JD, Beaver JD, Gunn RN, Nabulsi N, Weinzimmer D, Singhal T *et al* (2012). Affinity and selectivity of [(11) C]-(+)-PHNO for the D3 and D2 receptors in the rhesus monkey brain *in vivo*. *Synapse* **66**: 489–500.

Gerasimov MR, Franceschi M, Volkow ND, Rice O, Schiffer WK, Dewey SL (2000). Synergistic interactions between nicotine and cocaine or methylphenidate depend on the dose of dopamine transporter inhibitor. *Synapse* **38**: 432–437.

Ginovart N, Galineau L, Willeit M, Mizrahi R, Bloomfield PM, Seeman P *et al* (2006). Binding characteristics and sensitivity to endogenous dopamine of [^{11}C]-(+)-PHNO, a new agonist radiotracer for imaging the high-affinity state of D2 receptors *in vivo* using positron emission tomography. *J Neurochem* **97**: 1089–1103.

Ginovart N, Willeit M, Rusjan P, Graff A, Bloomfield PM, Houle S *et al* (2007a). Positron emission tomography quantification of [^{11}C]-(+)-PHNO binding in the human brain. *J Cereb Blood Flow Metab* **27**: 857–871.

Ginovart N, Willeit M, Rusjan P, Graff A, Bloomfield PM, Houle S *et al* (2007b). Positron emission tomography quantification of [^{11}C]-(+)-PHNO binding in the human brain. *J Cereb Blood Flow Metab* **27**: 857–871.

Girgis RR, Xu X, Miyake N, Easwaramoorthy B, Gunn RN, Rabiner EA *et al* (2011). *In vivo* binding of antipsychotics to D(3) and D(2) receptors: a PET study in baboons with [(11)C]-(+)-PHNO. *Neuropsychopharmacology* **36**: 887–895.

Gunn RN, Gunn SR, Turkheimer FE, Aston JAD, Cunningham VJ (2002). Positron emission tomography compartmental models: a basis pursuit strategy for kinetic modeling. *J Cereb Blood Flow Metab* **22**: 1425–1439.

Hauber W, Fuchs H (2000). Dopamine release in the rat globus pallidus characterised by *in vivo* microdialysis. *Behav Brain Res* **111**: 39–44.

Hwang DR, Kegeles LS, Laruelle M (2000). (−)-N-[(11)C]propylnorapomorphine: a positron-labeled dopamine agonist for PET imaging of D(2) receptors. *Nucl Med Biol* **27**: 533–539.

Ichise M, Ballinger JR, Golan H, Vines D, Luong A, Tsai S *et al* (1996). Noninvasive quantification of dopamine D2 receptors with iodine-123-IBF SPECT. *J Nucl Med* **37**: 513–520.

Ichise M, Cohen RM, Carson RE (2008). Noninvasive estimation of normalized distribution volume: application to the muscarinic-2 ligand [(18)F]FP-TZTP. *J Cereb Blood Flow Metab* **28**: 420–430.

Ichise M, Toyama H, Innis RB, Carson RE (2002). Strategies to improve neuroreceptor parameter estimation by linear regression analysis. *J Cereb Blood Flow Metab* **22**: 1271–1281.

Imperato A, Mulas A, DiChiara G (1986). Nicotine preferentially stimulates dopamine release n the limbic system of freely moving rats. *Eur J Pharmacol* **132**: 337–338.

Innis RB, Cunningham VJ, Delforge J, Fujita M, Gjedde A, Gunn RN *et al* (2007). Consensus nomenclature for *in vivo* imaging of reversibly binding radioligands. *J Cereb Blood Flow Metab* **27**: 1533–1539.

Lammertsma AA, Hume SP (1996). Simplified reference tissue model for PET receptor studies. *NeuroImage* **4**(Part 1): 153–158.

Laruelle M (2000). Imaging synaptic neurotransmission with *in vivo* binding competition techniques: a critical review. *J Cereb Blood Flow Metab* **20**: 423–451.

Logan J, Fowler JS, Volkow ND, Wang GJ, Ding YS, Alexoff DL (1996). Distribution volume ratios without blood sampling from graphical analysis of PET data. *J Cereb Blood Flow Metab* **16**: 834–840.

Logan J, Fowler JS, Volkow ND, Wolf A, Dewey SL, Schlyer D *et al* (1990). Graphical analysis of reversible radioligand binding from time-activity measurements applied to [N-^{11}C-methyl]-(−)-cocaine PET studies in human subjects. *J Cereb Blood Flow Metab* **10**: 740–747.

Marenco S, Carson RE, Berman KF, Herscovitch P, Weinberger DR (2004). Nicotine-induced dopamine release in primates measured with [^{11}C]raclopride PET. *Neuropsychopharmacology* **29**: 259–268.

Marshall DL, Redfern PH, Wonnacott S (1997). Presynaptic nicotinic modulation of dopamine release in the three ascending pathways studied by *in vivo* microdialysis: comparison of naive and chronic nicotine-treated rats. *J Neurochem* **68**: 1511–1519.

Mizrahi R, Houle S, Vitcu I, Ng A, Wilson AA (2010). Side effects profile in humans of (11)C-(+)-PHNO, a dopamine D(2/3) agonist ligand for PET. *J Nucl Med* **51**: 496–497.

Montgomery AJ, Lingford-Hughes AR, Egerton A, Nutt DJ, Grasby PM (2007). The effect of nicotine on striatal dopamine release in man: a [^{11}C]raclopride PET study. *Synapse* **61**: 637–645.

Morris E, Kim S, Sullivan J, Wang S, Normandin M, Constantinescu C *et al* (2013). Creating dynamic images of short-lived dopamine fluctuations with lp-ntPET: dopamine movies of cigarette smoking. *JoVE*. doi:10.3791/50358.

Narendran R, Slifstein M, Guillin O, Hwang Y, Hwang DR, Scher E *et al* (2006). Dopamine (D2/3) receptor agonist positron emission tomography radiotracer [^{11}C]-(+)-PHNO is a D3 receptor preferring agonist in vivo. *Synapse* **60**: 485–495.

Paxinos G, Huang X, Toga A (2000). *The Rhesus Monkey Brain in Stereotaxic Coordinates*. Academic Press: San Diego, CA.

Sandiego CM, Weinzimmer D, Carson RE (2013). Optimization of PET-MR registrations for nonhuman primates using mutual information measures: a Multi-Transform Method (MTM). *NeuroImage* **64**: 571–581.

Scott DJ, Domino EF, Heitzeg MM, Koeppe RA, Ni L, Guthrie S *et al* (2007). Smoking modulation of mu-opioid and dopamine D2 receptor-mediated neurotransmission in humans. *Neuropsychopharmacology* **32**: 450–457.

Shim I, Javaid JI, Wirtshafter D, Jang SY, Shin KH, Lee HJ *et al* (2001). Nicotine-induced behavioral sensitization is associated with extracellular dopamine release and expression of c-Fos in the striatum and nucleus accumbens of the rat. *Behav Brain Res* **121**: 137–147.

Shotbolt P, Tziortzi AC, Searle GE, Colasanti A, van der Aart J, Abanades S *et al* (2012). Within-subject comparison of [(11)C]-(+)-PHNO and [(11)C]raclopride sensitivity to acute amphetamine challenge in healthy humans. *J Cereb Blood Flow Metab* **32**: 127–136.

Slifstein M, Kegeles LS, Xu X, Thompson JL, Urban N, Castrillon J *et al* (2010). Striatal and extrastriatal dopamine release measured with PET and [(18)F] fallypride. *Synapse* **64**: 350–362.

Sullivan J, Kim S, Cosgrove K, Morris E (2013). Limitations of SRTM, logan graphical method, and equilibrium analysis for measuring transient dopamine release with [^{11}C]raclopride PET. *Am J Nucl Med Mol Imag* **3**: 247–260.

Takahashi H, Fujimura Y, Hayashi M, Takano H, Kato M, Okubo Y *et al* (2007). Enhanced dopamine release by nicotine in cigarette smokers: a double-blind, randomized, placebo-controlled pilot study. *Int J Neuropsychopharmacol* **11**: 1–5.

Talhout R, Opperhuizen A, van Amsterdam JG (2007). Role of acetaldehyde in tobacco smoke addiction. *Eur Neuropsychopharmacology* **17**: 627–636.

Tsukada H, Miyasato K, Kakiuchi T, Nishiyama S, Harada N, Domino EF (2002). Comparative effects of methamphetamine and nicotine on the striatal [(11)C]raclopride binding in unanesthetized monkeys. *Synapse* **45**: 207–212.

Tziortzi AC, Searle GE, Tzimopoulou S, Salinas C, Beaver JD, Jenkinson M *et al* (2011). Imaging dopamine receptors in humans with [^{11}C]-(+)-PHNO: dissection of D3 signal and anatomy. *Neuroimage* **54**: 264–277.

Villegier AS, Lotfipour S, McQuown SC, Belluzzi JD, Leslie FM (2007). Tranylcypromine enhancement of nicotine self-administration. *Neuropharmacology* **52**: 1415–1425.

Willeit M, Ginovart N, Graff A, Rusjan P, Vitcu I, Houle S *et al* (2008). First human evidence of *d*-amphetamine induced displacement of a D2/3 agonist radioligand: a [^{11}C]-(+)-PHNO positron emission tomography study. *Neuropsychopharmacology* **33**: 279–289.

Willeit M, Ginovart N, Kapur S, Houle S, Hussey D, Seeman P *et al* (2006). High-affinity states of human brain dopamine D2/3 receptors imaged by the agonist [^{11}C]-(+)-PHNO. *Biol Psychiatry* **59**: 389–394.

Wilson AA, McCormick P, Kapur S, Willeit M, Garcia A, Hussey D *et al* (2005). Radiosynthesis and evaluation of [^{11}C]-(+)-4-propyl-3,4,4a,5,6,10*b*-hexahydro-2*H*-naphtho[1,2-*b*][1,4]oxazin-9-ol as a potential radiotracer for *in vivo* imaging of the dopamine D2 high-affinity state with positron emission tomography. *J Med Chem* **48**: 4153–4160.

Supplementary Information accompanies the paper on the Neuropsychopharmacology website (http://www.nature.com/npp)